

# FINITE ELEMENT ANALYSIS ON HELIUM DISCHARGE IN THE STORAGE RING TUNNEL

J.C. Chang, J.C. Huang, Y.C. Chang, F.Z. Hsiao, S.P. Kao, H.C. Li, W.R. Liao, and C.Y. Liu  
National Synchrotron Radiation Research Center, Hsinchu, Taiwan

## Abstract

Liquid helium for transferring cooling power from the cryogenic plant to the magnets and SRF cavities had been widely applied on the advanced large superconducting particle accelerators. For requirements of high stable and reliable operation, many efforts have been put into the improvement and modification of the cryogenic system. However, personnel safety is another critical issue of the cryogenic system. Once large liquid helium was released on the atmospheric tunnel, the volume of helium will expand several hundred times and cause oxygen deficiency in short time due to sudden change of helium density. In this study, we applied numerical simulation to analyse helium discharge through a SRF cavity in the TPS tunnel.

Personnel safety is another critical issue of the cryogenic system. Once large liquid helium (LHe) was released on the atmospheric tunnel, the volume of helium will expand several hundred times in short time due to sudden change of its density. Therefore, cold helium discharge test in the LHC tunnel at CERN had been experimentally conducted. [2] Numerical simulation of cold helium safety discharges had also been performed at European Spallation Source (ESS). [3] We also had performed numerical analysis to simulate the worst case of helium discharge through a SRF cavity in the TPS ring tunnel. A small experiment was conducted to validate the numerical simulation. [4] In this study, we analysed more possible cases of helium discharge in the TPS tunnel.

## INTRODUCTION

National Synchrotron Radiation Research Center in Taiwan (NSRRC) had set up three cryogenic systems to provide liquid helium to superconducting radio-frequency (SRF) cavities, insertion devices, and highly brilliant hard X-ray. The first one could produce liquid helium 134 LPH, with maximum cooling capacity of 469 W at 4.5 K. The second one could produce liquid helium 138 LPH, with maximum cooling capacity of 475 W at 4.5 K. The third one could produce liquid helium 239 LPH, with maximum cooling capacity of 890 W at 4.5 K. However, large liquid helium discharge in a closed space will cause personnel danger of lack of oxygen. We performed Computational Fluid Dynamic (CFD) simulation to analyse helium discharge through a SRF cavity in the Taiwan Light Source (TPS) tunnel. We simulated cases of helium discharge flow rates from 0.1 kg/s to 4.2 kg/s with and without fresh air supplied from the air conditioning system. We also set up both physical and numerical models within a space of 2.4m in length, 1.2m in width and 0.8m in height with nitrogen discharge inside to validate the CFD simulation.

One cryogen distribution system has been installed and commissioned to transfer liquid nitrogen and LHe from storage dewars to superconducting radio-frequency (SRF) cavities at TPS. [1] The cryogenic system has maximum cooling capacity 890 W with associated compressors, an oil-removal system, four helium buffer tanks, one 7000-L Dewar, gaseous helium piping at room temperature, transfer lines to distribute helium, and a transfer system for liquid nitrogen. Currently, there are two SRF cavities are located one upstream and one downstream of the distribution valve box.

## NUMERICAL SIMULATION

CFD began from the early 30s of the 20th century to solve the linearized potential equations with 2D methods (1972). As rapid development of numerical analysis and computer science, CFD has more advantage of well adaptation than traditional theoretical analysis and experimental measurements. Nowadays, CFD has been widely applied in many fields. Detailed 3D numerical simulation was performed using a commercial general purpose CFD code ANSYS Fluent.

### Governing Equation

We set our simulated model as a 3D turbulent flow in this study. The basic governing equations include the continuity equation, the momentum equation and the energy equation.

We apply the k-ε turbulence model and SIMPLEC to solve the velocity and pressure problem.

Mass conservation equation (continuity equation)

$$\frac{\partial \rho}{\partial t} + \nabla \cdot (\rho \mathbf{u}) = 0 \quad (1)$$

where  $\rho$  is density of fluid,  $t$  is time and  $\mathbf{u}$  refers to fluid velocity vector.

Momentum conservation equation

$$\frac{\partial (\rho \mathbf{u})}{\partial t} + \nabla \cdot (\rho \mathbf{u} \mathbf{u}) = -\nabla p + \rho \mathbf{g} + \nabla \cdot (\mu \nabla \mathbf{u}) - \nabla \cdot \tau_t \quad (2)$$

where  $p$  is pressure,  $\mathbf{g}$  is vector of gravitational acceleration,  $\mu$  is dynamic viscosity of fluid, and  $\tau_t$  is divergence of the turbulent stresses which accounts for auxiliary stress due to velocity fluctuations.

Energy conservation equation

$$\frac{\partial (\rho e)}{\partial t} + \nabla \cdot ((\rho e + p) \mathbf{u}) = \nabla \cdot \left( k \nabla T - \sum_j h_j \mathbf{j}_j \right) \quad (3)$$

where  $e$  is the specific internal energy,  $T$  is fluid temperature,  $k$  is heat conductivity,  $h$  is the specific enthalpy of fluid,  $\mathbf{j}$  is the mass flux. In this study, RNG (Re-Normalisation Group)  $\kappa$ - $\epsilon$  turbulent model was used.

### Geometry and Grid Generation

A detailed 3D model of 2 of 24 sections of the TPS tunnel, where a SRF cavity is located, was built for the numerical simulation. The space of the simulation zone is about 860.5 m<sup>3</sup>. Magnets and girders are simplified as a continuous rectangular solid in the tunnel. The geometry was built according to the dimensions of the tunnel, as shown in Fig.1. We also take the effects of the air conditioning system into simulation. Supplied air exits and two air exhausts are distributed on overhead of the inner wall. There is one exhaust blower installed on the inner wall near the helium discharge exit.

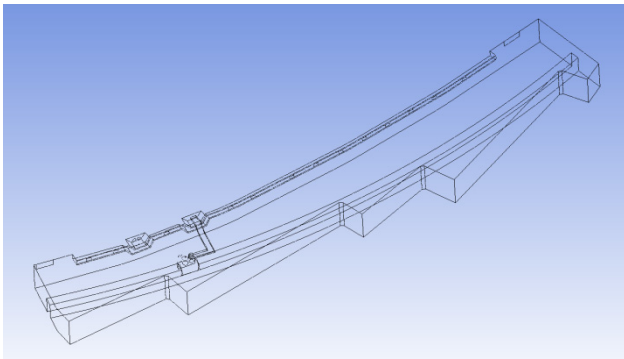


Figure 1: Numerical model of 2 sections of TPS.

According to the geometry of the model, we applied hybrid grid to discretize the model. The total number of the grid elements was about 3.34 million. To more accurately analyse the flow fields and greater control over sizing function, we applied the Advanced Size Function. The size of relevance center was fine. The minimum grid element size is 0.00177m near the helium discharge exit. Figure 2 shows the generated grids of the numerical simulation.

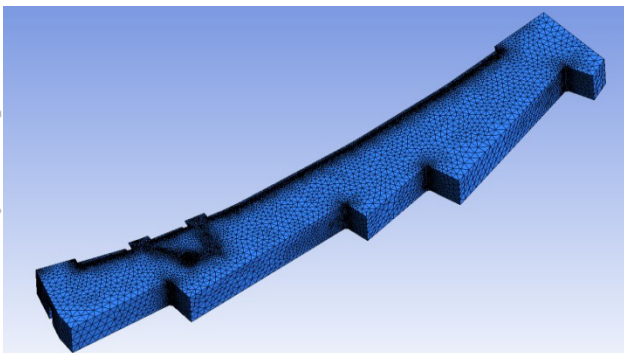


Figure 2: Generated grids of the numerical model.

### Initial and Boundary Conditions

The flowrate of helium discharge was given the case of 0.5 kg/s. Time of helium discharge is 120 s. There are

two simulation cases A and B in this study. Case A: Discharge helium flows vertically upward. Case B: Discharge helium flowing toward the exhaust blower on inner wall. Other initial and boundary conditions are list as follow.

1. Air temperature in the tunnel is 25 °C at  $t = 0s$ .
2. Discharged helium temperature is 4 K.
3. Wall and floor are adiabatic.
4. Both sides are opened to atmosphere (1atm).
5. Supplied air flow velocity is 2 m/s from air exits.
6. Back pressure of the air exhaust is 1000pa.

## RESULTS AND DISCUSSION

We select three monitor planes P1, P2, and P3 respectively at  $z = 1.5m$ ,  $2.8m$  and the cross sectional plane through the exhaust blower. In this study, we analysed the helium mass fraction. Once helium mass fraction is over 2.26%, the oxygen concentration is less than 18%. Figure 3 shows the simulation results of helium mass fraction of cases A on P1 and P3 at  $t = 30s$ .

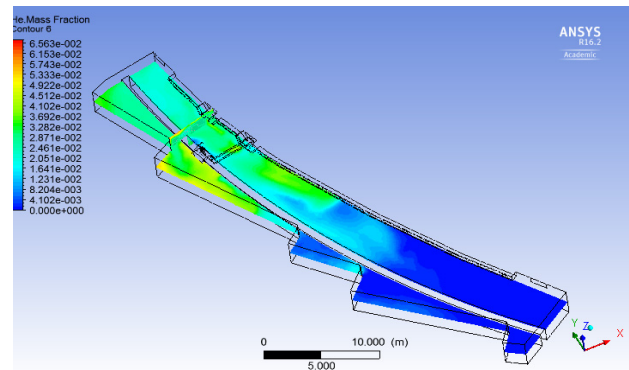


Figure 3: Simulation results of helium mass fraction of case A on P1 and P3 at  $t = 30s$ .

The simulated helium mass fraction is distributed from 6.563% to 0%. It can be observed that the helium mass fraction of left upper area is higher than that of right lower area due to the helium discharge position. Higher helium mass fraction is shown on the wedge area near the outer wall because that a circulation forms in that area.

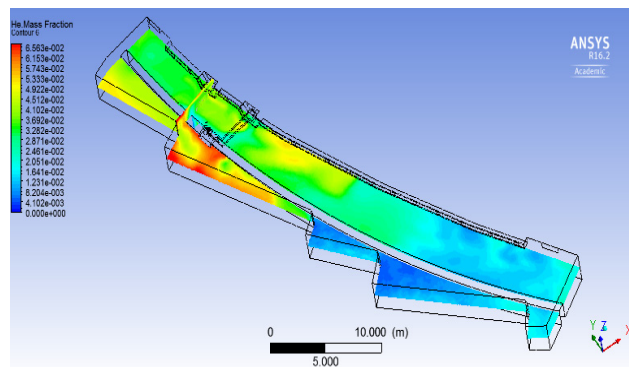


Figure 4: Simulation results of helium mass fraction of case A on P1 and P3 at  $t = 60s$ .

Figure 4 shows the simulation results of helium mass fraction of case A on P1 and P3 at  $t = 60s$ . The helium mass fractions of both cases at  $t = 60s$  are clearly higher than that at  $t = 30s$  in Fig. 3. Some helium remaining on the wedge area near the outer wall is clearer. Through the helium mass fraction distribution on the P3, it is shown that the helium mass fraction is high near the ceiling.

Figure 5 shows the simulation results of helium mass fraction of case A on P2 at  $t = 60s$ . The helium mass fractions on P2 are clearly higher than that on P1 in Fig. 4. Air flowing profile through the air exits is also clearly shown in Fig. 5.

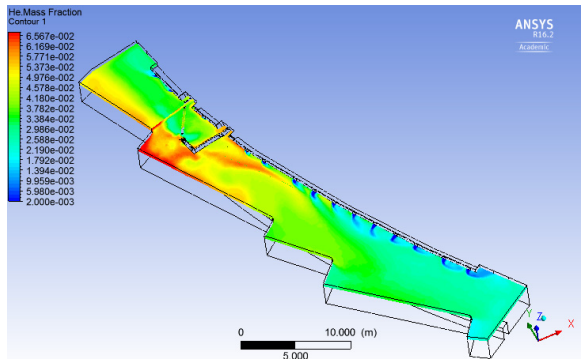


Figure 5: Simulation results of helium mass fraction of case A on P2 at  $t = 60s$ .

Figure 6 shows the simulation results of helium mass fraction of case B on P1 and P3 at  $t = 60s$ . Because discharge helium flowing toward the exhaust blower on inner wall, the helium mass fraction is lower than that of case A, as shown in Fig. 4 and 6. As the exhaust blower is installed on high place in the inner wall, the helium mass fraction is lower near the ceiling, as shown on P3 in Fig. 6.

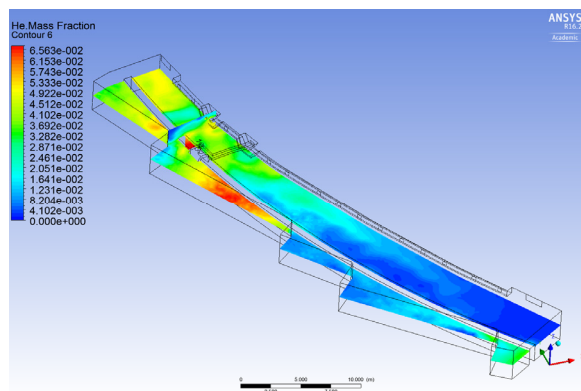


Figure 6: Simulation results of helium mass fraction of case B on P1 and P3 at  $t = 60s$ .

Figure 7 shows the simulation results of helium mass fraction of case A on P2 at  $t = 60s$ . The helium mass fractions on P2 are clearly higher than that on P2 in Fig.5 except the region near the exhaust blower. Air flowing profile through the air exits is also clearly shown in Fig. 7.

Figure 8 shows histories of simulation results of helium mass fraction of case A on points 1 and 2, which respectively locate near the helium exit and the exhaust

blower. Only in start few second, helium mass fraction on point 2 is higher than that on point 2.

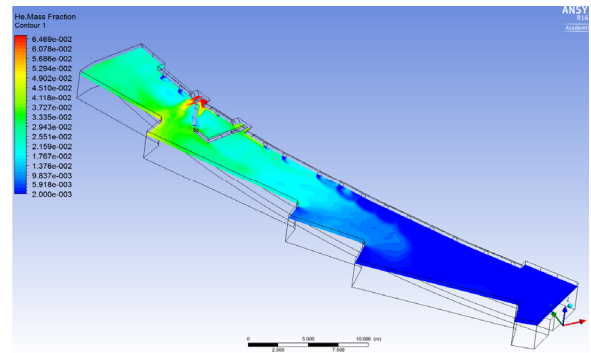


Figure 7: Simulation results of helium mass fraction of case B on P2 at  $t = 60s$ .

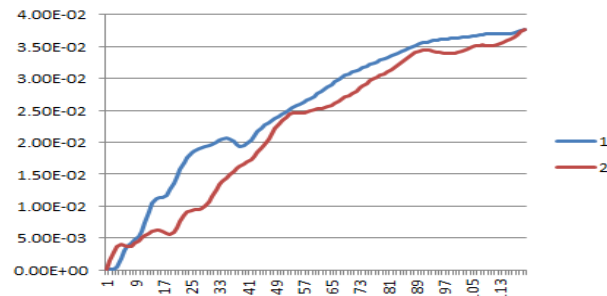


Figure 8: Histories of simulation results of helium mass fraction of case A on points 1 and 2.

### CONCLUSION AND FUTURE WORKS

We performed CFD simulation to analyse cases A and B of helium discharge through a SRF cavity in the TPS tunnel. It shows that case B, discharge helium flowing toward the exhaust blower, may effectively decrease the helium concentration. We will perform CFD simulation to analyse nitrogen discharge in a hutch in near future.

### ACKNOWLEDGEMENT

Authors would like to thank colleagues in the utility and civil, RF, Cryogenic group and Safety division of NSRRC for their assistance.

### REFERENCES

- [1] H.H. Tsai *et al.*, "Installation and commissioning of a cryogen distribution system for the TPS project", *Cryogenics*, Volume 77, July 2016, Pages 59–64.
- [2] L. Dufay-Chanat *et al.*, "Final report on the Controlled Cold Helium Spill Test in the LHC tunnel at CERN", IOP Conf. Series: Materials Science and Engineering 101, 2015.
- [3] R. Andersson *et al.*, "Numerical simulation of cold helium safety discharge into a long relief line", 25th International Cryogenic Engineering Conference and the International Cryogenic Materials Conference, University of Twente, Enschede, Netherlands, 2014.
- [4] J.C. Chang *et al.*, "Experimental validated CFD analysis on helium discharge", in *Proc. MEDSI 2016*, Barcelona, Spain, Sep. 2016.